First-principles calculations of hyperfine fields in the $CeIn_3$ intermetallic compound

M. V. Lalić,* J. Mestnik-Filho,† A. W. Carbonari, and R. N. Saxena
Instituto de Pesquisas Energéticas e Nucleares, CP 11049, 05422-970 São Paulo, SP, Brazil

H. Haas
Bereich Festkörperphysik, Hahn-Meitner-Institut Berlin, D-14109 Berlin, Germany

(Received 26 January 2001; revised manuscript received 26 April 2001; published 27 December 2001)

The first-principles full potential linear augmented plane-wave calculations of the electronic structure and hyperfine fields have been performed for $CeIn_3$ compound in the antiferromagnetic phase. Cerium $4f$ states, positioned at the Fermi level, have been treated inside the valence panel, interacting with the other valence states. The calculated values of hyperfine fields both at Ce and In sites are found to be in reasonable agreement with the lowest-temperature measurements. The $4f$ orbital contribution dominates the magnetic hyperfine field (MHF) at the Ce sites. The contact field is negligible due to an almost complete cancellation of valence and core contributions. A nonzero MHF appears at In sites despite the fact that no net magnetic moment is induced and the vector sum of the nearest-neighbor Ce magnetic moments is zero. The $5p$ subshells of In are spin polarized due to the hybridization with the extended Ce valence states. This polarization is essential for the appearance of a small MHF at the In nucleus, which has mostly a spin-dipolar character. The $5p$ shell of In is also responsible for the presence of an electric-field gradient (EFG) at In nucleus in $CeIn_3$. The $5p$ subshell polarization, however, does not influence this EFG as it is developed mainly in the region closer to the nucleus, where the spin ''up'' and spin ''down'' $5p$ subshells show no difference.

DOI: 10.1103/PhysRevB.65.054405 PACS number(s): 76.80.+y, 71.20.Eh, 75.20.Hr

I. INTRODUCTION

During the last decades considerable attention has been focused on the nature of the ground state of cerium-based compounds and alloys. The reason for such interest lies in the fact that many physical phenomena, such as ferro- and antiferromagnetism, Kondo effect, superconductivity, intermediate valence, and heavy fermion behavior, can take place in these Ce systems.[1–3] Having an open $4f$ shell, the Ce ion possesses a permanent magnetic moment, which has a tendency to be preserved in the crystalline environment, due to small spatial extension of f states and their efficient screening by the outer conduction electrons. These f moments are coupled to each other via intersite Ruderman-Kittel-Kasuya-Yosida (RKKY) interaction, giving rise to various kinds of magnetic ordering. On the other hand, since the Ce $4f$ level lies close to the Fermi energy, f moments are subjected to the on-site Kondo interaction, which tends to suppress the magnetic order. In many Ce-based materials competition between these two interactions determines the nature and properties of the ground state.

In $CeIn_3$, RKKY interaction prevails and the compound is ordered antiferromagnetically below $T_N = 10.2$ K. The neutron-scattering study[4] showed the Ce magnetic moments to be aligned in opposite directions in the neighboring (111) planes although the precise direction of the moments could not be determined. It has been found[5] that the substitution of a small fraction of In atoms by Sn destroys the magnetism, indicating that the ground-state parameters in $CeIn_3$ lie near the critical values at which instability of Ce $4f$ moment occurs. Recently, $CeIn_3$ was also shown to exhibit superconductivity which appears under a pressure of about 2.5 GPa.[6] These observations, together with the fact that $CeIn_3$ shows heavy fermion behavior at low temperatures, makes this compound an interesting system to investigate.

In this paper we will focus our attention on the hyperfine fields (HF's) acting in the intermetallic compound $CeIn_3$. HF's are important quantities that characterize the crystalline ground state and offer the information about the electronic charge and spin distribution in the immediate vicinity of nuclear positions. In $CeIn_3$, the HF's have not yet been calculated theoretically, most probably due to the fact that reliable experimental data became available only very recently. The HF's in $CeIn_3$ were measured in the last two years, using time differential perturbed angular correlation (TDPAC) and nuclear quadrupole resonance (NQR) techniques.

In the TDPAC study,[7] the MHF at ^{140}Ce as well as the MHF and electric-field gradient (EFG) at ^{111}Cd nuclei dilutely substituting the In sites have been measured as a function of temperature, down to 7 K. Very recently the result of a TDPAC measurement at 4.2 K also became available[8] which gave a value of 32.9 ± 0.1 T for the MHF at Ce site. No electric quadrupole interaction is expected at the Ce position due to its cubic environment.

The hyperfine interactions in $CeIn_3$ were also measured using ^{115}In NQR.[9] The measurements, which were performed at 4.2 K, provided complementary information about the hyperfine fields acting on the In nuclei (not on a ^{111}Cd impurity at In site as in the TDPAC experiments). A hyperfine field of the order of 0.4–0.5 T acting on In nuclei was determined. From the reported lowest transition frequency $\nu_Q = 9.6$ MHz, corresponding to the $|\pm 3/2\rangle \leftrightarrow |\pm 5/2\rangle$ sublevel excitations, we calculated the value of EFG giving $V_{zz} = 11.6 \times 10^{21}$ V/m^2. The value of quadrupole moment $Q = 0.83b$,[10] for ^{115}In, was used for this calculation.

Motivation for the present work was to discuss and try to provide an interpretation of these experimental data. For this purpose we have calculated the electronic structure of the $CeIn_3$ compound and the HF's in its antiferromagnetic phase,

using the full potential linear augmented plane-wave (FP-LAPW) method.[11] In the analysis of the results, especial attention has been devoted to the questions that could not be answered by the experiments: (i) Which contribution, contact, orbital, or spin-dipolar, dominates the MHF's at both Ce and In sites? (ii) What is the origin of a nonzero MHF at In sites? (iii) Which electrons contribute most to the EFG at In sites? (iv) Which states play an important role in hybridization processes that take place in the compound? The main objective of the present work is to clarify these questions from the electronic structure point of view.

II. CALCULATIONS

The intermetallic compound $CeIn_3$ has a cubic structure of the $AuCu_3$ prototype, with a lattice parameter of 4.690 Å.[12] The Ce atoms are located at the corners and the In atoms at the face-centered positions of a cubic unit cell (space group $Pm3m$). Since the Ce magnetic moments are aligned antiferromagnetically this unit cell has to be doubled in order to account for a difference between the spin ''up'' and spin ''down'' Ce atoms. The magnetic unit cell of $CeIn_3$ is also cubic with twice the value of the lattice parameter, but has a different symmetry (space group $Fm3m$). The spin up and spin down Ce ions are located at $4a$ and $4b$ positions, respectively, whereas the In atoms are situated at $24d$ sites in Wyckoff's notation.

In order to include the spin-orbit interaction in the calculations we had to impose some direction for the Ce magnetic moment. Various choices would generate different symmetries of the Hamiltonian, leading to different solutions in general. Since the Ce magnetic moment direction is not known from the experiment[4] we assumed it to be along (111), (110), and (100) axes of the magnetic unit cell and performed fully self-consistent calculations for the three cases under the same conditions. The total-energy differences were found to be within the fifth decimal place of the Rydberg scale, and hyperfine fields varied by less than 5%. It was thus not possible to determine the preferential Ce magnetic moment direction due to the weakness of the magnetic anisotropy in the system compared with interatomic exchange interaction.

We present here just one case in which the Ce spins are directed along the (111) axis. Starting from the cubic magnetic unit cell described above we chose a rhombohedral primitive unit cell with lattice parameter $a=6.633$ Å and $\gamma=60°$ (space group $R\bar{3}m$). The spin up and spin down Ce atoms are located at $1a$ and $1b$ positions, respectively, and In atoms at $3d$ and $3e$ positions, split in two nonequivalent groups because of the spin-orbit interaction term in the Hamiltonian. All the calculations presented here refer to this primitive unit cell.

Self-consistent band-structure calculations for $CeIn_3$ were performed using the WIEN97 computer code[13] which is based on the application of the FP-LAPW method. In this method, the electronic wave functions, the charge density, and the crystal potential are expanded in spherical harmonics inside the nonoverlapping spheres centered at each nuclear position (with radii R_{MT}), and in plane waves in the rest of the space (so-called interstitial region). We have chosen $R_{MT}=3.0$ a.u. for both Ce and In atomic sphere radii. Inside the atomic spheres, waves are expanded up to $l_{max}=6$, while the number of plane waves in the interstitial is limited by the cutoff at $k_{max}=8.5/R_{MT}$. The charge density was Fourier expanded up to $G_{max}=14$. For a Brillouin-zone integration, a mesh of 2000 $\vec{k}$ points in the whole zone was used (182 in its irreducible wedge). Exchange and correlation effects were treated within the density functional with generalized-gradient corrections (GGA96).[14] The following atomic states of Ce ($5s^25p^64f^15d^16s^26p^0$) and In ($4d^{10}5s^25p^1$) were considered as valence states. In the process of solving the Dirac's equation they are treated within the scalar-relativistic approach while the core states are relaxed in a fully relativistic manner. Spin-orbit interaction, important for the treatment of the Ce $4f$ shell, was calculated self-consistently in a wide energy window (~ 5 Ry) around the Fermi level. Calculation of MHF's, implemented into the WIEN97 code, was performed following formulas from Ref. 15, which include the relativistic corrections. In the scalar-relativistic approach the spin projection remains a good quantum number, while the spin-orbit interaction is treated in a second-variational procedure. Thus, throughout this paper, orbital and spin momenta, rather than total angular momentum J, will be used.

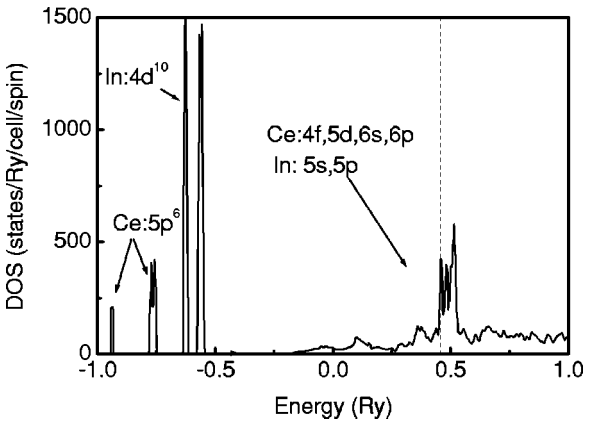

FIG. 1. Total density of states (DOS) for $CeIn_3$ compound, obtained by the FP-LAPW method. The dashed line indicates the Fermi level.

III. ELECTRONIC STRUCTURE

The calculated density of states (DOS) for $CeIn_3$ is presented in Fig. 1 showing states in a broad energy interval around the Fermi level ($E_F=0.455$ Ry). All of the states included in the valence panel are present except the Ce $5s$ states which lie deeper at the energy of approximately -2 Ry. The Ce $5p$ and In $4d$ states remain atomiclike, positioned deep below E_F, but split due to the crystal-field perturbation. All the other states, $4f$, $5d$, $6s$, $6p$ from Ce and $5s$, $5p$ from In, are situated around the Fermi level, interacting and hybridizing among themselves.

The most important states are certainly the cerium $4f$ states (Fig. 2). Apart from the fact that they carry the majority of the magnetic moment in the compound, the contribution of these states to the DOS at the Fermi level is by far the

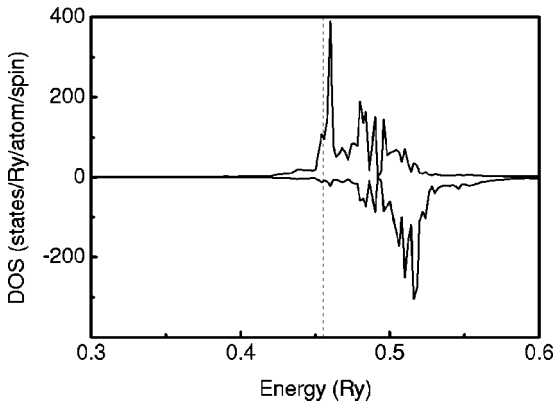

FIG. 2. Partial spin up and spin down DOS for Ce $4f$ states in the $CeIn_3$ compound, calculated by the FP-LAPW method. The dashed line indicates the Fermi level.

largest. The Ce 5d and the In $5p$ states have much smaller DOS at E_F while the Ce $6s$, $6p$, and the In $5s$ contributions are almost negligible.

The calculated spin magnetic moment at the Ce atom is found to be $0.708\mu_B$. The largest part of this moment is carried by the $4f$ shell ($0.639\mu_B$). Other Ce valence shells are also spin polarized due to the interaction with the $4f$ spin moment. The $6s$, $6p$, and $5d$ valence shells are characterized by spin moments of $0.003\mu_B$, $0.005\mu_B$, and $0.061\mu_B$, respectively. Unlike the $4f$ shell, these valence shells have spatial extension and are capable of transferring the magnetic moment to the neighboring In atoms. In addition to the spin moment the Ce atom developed a significant orbital magnetic moment of $-0.531\mu_B$, originating almost completely from the $4f$ shell ($-0.528\mu_B$), with its direction opposite to the spin magnetic moment. The total magnetic moment on Ce is thus $0.177\mu_B$. Lawrence *et al.*[4] reported a value of $0.65\pm0.1\mu_B$ from their neutron-diffraction measurement at $T=5$ K, while Benoit *et al.*[12] determined a value of $0.48\pm0.08\mu_B$ also from neutron-diffraction study at $T=3$ K. As can be seen the agreement between the experimental value and the calculated result is rather poor. One of the reasons for this discrepancy is the tendency of the local-density approximation (LDA) to underestimate the orbital moment.[16] It is possible that the GGA also suffers from the same kind of problem. Another source of error in orbital moment calculation can be a non-self-consistent treatment of the orbital polarization. Finally, the errors in both orbital and spin magnetic moments may come from the present treatment of Ce $4f$ states. The use of self-interaction correction (SIC),[17] or LDA+U (Ref. 18) corrections for these states, might improve the agreement with experiment.

No net magnetic moment is found at the In position due to the fact that In $5s$ and $5p$ valence states do not exhibit any spin polarization. While this statement is completely true for $5s$ shell, the situation for the $5p$ shell is more complex. Although the complete $5p$ shell is equally populated by the spin up and spin down electrons so that the resulting magnetic moment of the shell is zero, spin populations in its p_x, p_y, and p_z orbitals differ for spin up and spin down directions significantly by 0.006, 0.004, and -0.010 electrons,

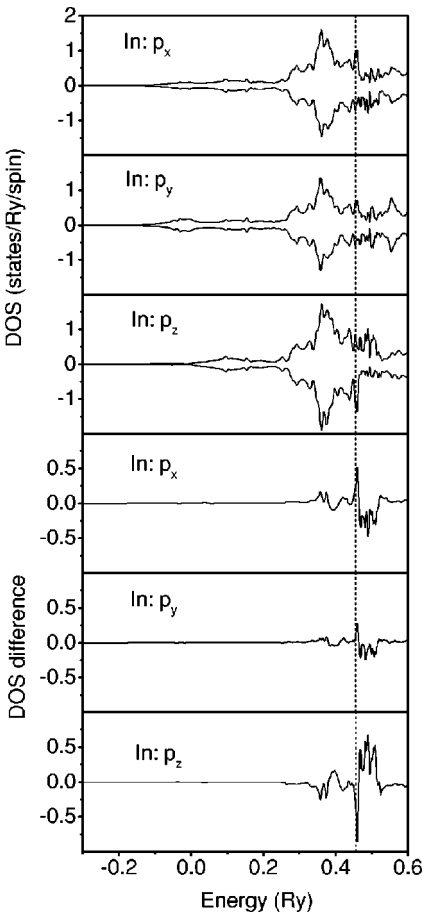

FIG. 3. Partial spin up and spin down DOS for In $5p_{x,y,z}$ states in $CeIn_3$ compound, obtained by the FP-LAPW method. Lower pictures show the differences between corresponding spin up and spin down densities.

respectively. These differences can be seen from the corresponding DOS shown in Fig. 3 and they occur only in the vicinity of the Fermi level while the DOS having lower energy remain unaffected. The wave functions describing the In $5p$ subshells differ in their energy dependence as well as in the energy dependence for spin up and down states. The same is valid for their spatial dependence. Thus, unlike the $5p$ shell as a whole, the $5p$ subshells are spin polarized, due to different energy and spatial distribution of spins. The reason for this polarization is the existence of a stable $4f$ magnetic moment on the Ce atom. Since the Ce $4f$ shell has a small radial extension, direct overlap with the $5p$ shell of In is not likely. Instead, the $4f$ moment polarizes the more extended $6s$, $6p$, and $5d$ valence states of Ce and these hybridize with the $5p$ shells of neighboring In atoms causing the polarization of their subshells. This effect is found to be responsible for the appearance of a small MHF at the In nuclei, as will be shown later.

The occupation numbers of specific orbitals will not be presented here since these quantities depend on the choice of atomic sphere radii. However, it should be mentioned that one of the important results was that the Ce $4f$ shell occupation remained almost the same as in the starting free-atom configuration even though this state is allowed to hybridize

TABLE I. Comparison of present FP-LAPW results for MHF's in $CeIn_3$ compound with the experimental values. Experimental value for Ce is taken from the TDPAC measurements at 4.2 K,[8] while for In from the NQR measurements at 4.2 K.[9] Signs of MHF's were not measured in these experiments. The decomposition of the theoretical MHF's is also presented.

	MHF (T) experiment	MHF (T) FP-LAPW	Contact field (T)	Orbital field (T)	Spin-dipolar field (T)
Ce	32.9 ± 0.1	-25.05	2.20	-27.74	0.49
In	0.4–0.5	-0.91	-0.04	-0.16	-0.71

with the other states. The resulting excess of 0.039 electrons is very small compared with the much more significant changes suffered by the other valence states. This is in agreement with the experimental observation that in $CeIn_3$ the $4f$ shell keeps nearly integral occupation ($n_f \rightarrow 1$) up to the lowest temperatures.[5]

IV. MAGNETIC HYPERFINE FIELDS

Magnetic hyperfine fields result from an interaction between the nuclear magnetic dipole moment and extra nuclear magnetic field generated by the electronic surrounding of the nucleus in the crystal. The MHF can arise from the spin-polarized charge density of *s*- or relativistic $p_{1/2}$ electrons at the nuclear position (contact field), due to the orbital magnetic moment of open electronic shells (orbital field), and due to the electronic spins (spin-dipolar field).

FP-LAPW results for the MHF's in $CeIn_3$ are presented in Table I. The Ce and In atoms shown are in positions (0,0,0) and (1/2,0,0), respectively. Other positions exhibit opposite signs for MHF's, so that in the complete unit cell the resulting MHF is zero. The fact that all In positions exhibit the same magnitude of MHF comes as a consequence of symmetry, i.e., from our choice of the direction of the magnetization axis.

A. Cerium position

As can be seen from the Table I, the MHF at the Ce site is dominated by the orbital contribution originating almost entirely from Ce $4f$ shell (-27.66 T). The situation is similar for the spin-dipolar field, although the field itself is much smaller. The contact field, which usually dominates the MHF in the case of *d*-shell magnetism, is surprisingly small here despite an evident polarization of Ce $6s$ valence shell.

A small contact field results from the cancellation of the valence and the core electron contributions, both of which are proportional to the local magnetic moment but have opposite signs. The valence contribution arises from the $6s$ magnetic moment ($0.003\mu_B$) inside the Ce atomic sphere, resulting in the excess of spin up DOS at the nuclear position, leading to a contact field of $+24.8$ T. The core contribution arises from the polarization of core *s*- and $p_{1/2}$ electrons, caused by the exchange interaction with the $4f$ local moment.[19] We obtained the value of -22.6 T for this contribution which when added to the valence contribution gave a contact field of 2.2 T as shown in Table I.

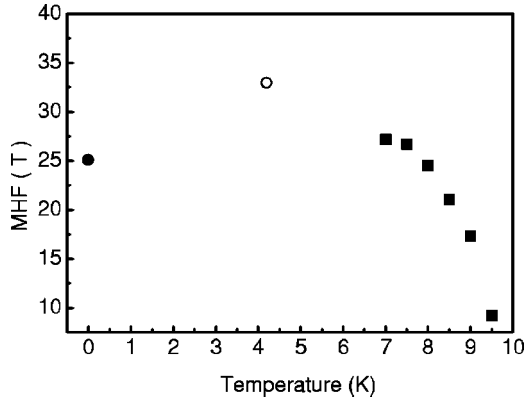

FIG. 4. Temperature dependence of MHF at the Ce nucleus in $CeIn_3$ antiferromagnetic phase, as measured by the TDPAC technique. Square symbols represent the results taken from Ref. 7. Empty circle is the new measurement from Ref. 8. MHF at $T=0$, denoted by a filled circle, is the FP-LAPW value.

A large value obtained for the orbital hyperfine field is not an unexpected result. Differently from the $3d$ and $4d$ compounds where strong crystal field frequently quenches the orbital angular momentum of the weakly shielded *d* shell and results in MHF mainly from the contact contribution, the $4f$ shell of Ce is efficiently shielded from the crystal field and the $4f$ orbital angular momentum L is not fully quenched giving rise to a large orbital field. What is less expected is the fact that the calculated $4f$ orbital field at Ce in $CeIn_3$ is almost seven times smaller than the value calculated for free trivalent Ce^{3+} ion which is known to be 192 T.[20] Because of the shielding effect mentioned above, it is generally believed that properties of the $4f$ electrons in crystal should differ very little from those of free ions. MHF measurement of dilute rare earths in insulators by electron spin resonance technique,[21] for example, confirm this behavior. The measured fields differ from the calculated free-ion values by less than 15% for the whole $4f$ series.[20] In $CeIn_3$ the discrepancy between the crystalline and free-ion $4f$ orbital field at the Ce nucleus is, however, too large. This leads to the conclusion that Ce $4f$ shell in $CeIn_3$ changes significantly in comparison with the $4f$ shell in the free ion. Two effects are responsible for this change: crystal-field influence ($4f$ electron not as efficiently screened as would be expected) and hybridization of the $4f$ shell with the other valence shells. Both effects change the spatial and energy distribution of electrons in $4f$ states and result in partial quenching of the orbital angular momentum of the shell.

The calculated value of MHF at the Ce site is compared with the experimental results in Fig. 4 where a temperature dependence of the measured MHF in the range of 10–4.2 K is shown. Strictly speaking, our calculations, based on density-functional theory (DFT), refer to a crystalline ground state and are valid for zero temperature only. However, DFT results can be (and often are) used to interpret the experimental data at finite temperatures. Since the present system is investigated in the antiferromagnetic regime, the calculated MHF should be used to discuss the experimental MHF in the

same regime. Even in real Kondo systems the DFT +LDA(GGA) calculated HF's are reliable enough to discuss the experimental situation at temperatures higher than Kondo temperature ($T > T_K$). In $CeIn_3$, moreover, T_K is expected to be very close to zero ($n_f \to 1$ implies $T_K \to 0$),[22] which means that all experimental MHF's shown in Fig. 4 correspond to long-range magnetic order. In this case, it is safe to compare our theoretical MHF with the MHF measured at temperatures $T \leqslant T_N/2$, T_N being the Néel temperature. The experimental MHF at $T = 4.2$ K fulfills this criterion, and we found its value to be in a reasonable agreement with the theoretical prediction (Table I).

The relatively good agreement between the theoretical and experimental Ce MHF's may be surprising in view of the fact that the agreement between the corresponding values of the magnetic moment is quite poor. The difficulty to trace the cause of this discrepancy increases from the fact that the calculated value of only the total magnetic moment can be compared with the experiment. Therefore there is no way of determining whether the spin or the orbital part of the magnetic moment is responsible for its disagreement with the experimental value. The fact that Ce MHF originates mostly from the orbital current suggests that the Ce orbital moment is probably determined correctly, and that the underestimation of the calculated total moment comes largely from the spin moment. However, an alternative explanation could be that Ce $4f$ wave function is determined more accurately in a region close to the nucleus rather than near the atomic sphere boundary. If this is the case then the Ce orbital MHF is calculated more accurately than the Ce orbital moment because the region very close to the nucleus is by far the most important for formation of the orbital MHF.

B. Indium position

The present FP-LAPW calculations give a small but nonzero value for the MHF at the In site. This is in agreement with the experimental findings. On the other hand, In atoms are found to have no local magnetic moment and situated at the symmetrical lattice positions in which the sum of the neighboring Ce magnetic moments is zero. Therefore the usual mechanism to account for the transferred MHF on a diamagnetic atom in a magnetic crystal may be excluded.

The contribution that dominates the MHF at In sites is spin dipolar. A small fraction also comes from the orbital contribution while the contact field is negligible (Table I). The nearly zero value for the contact field is not the consequence of cancellation of large contributions from valence and core electrons as is the case for Ce atoms. Both contributions are extremely small: the valence contribution, because there is no polarization of the In $5s$ shell, and the core contribution, because of the lack of polarization of the In core states since there is no moment in the valence shells which could cause it. We found that both spin-dipolar and orbital fields originate completely from In $5p$ valence shell. It was mentioned earlier that this shell does not carry any resultant magnetic moment although its subshells are spin-polarized. This polarization of $5p$ subshells is the reason why MHF appears at In nuclei. To further explain this point we must invoke the formulas for orbital and spin-dipolar contributions of MHF from Ref. 15.

The energy of interaction between electronic orbital magnetic moment and nuclear moment is given by the following expression:

$$E_{orb} = \frac{e}{mc}\vec{M}\left\langle \Phi \left| \frac{S(\vec{r},\epsilon)}{r^3}\vec{L} \right| \Phi \right\rangle, \tag{1}$$

while the interaction of electronic spin with the nuclear moment is characterized by the energy

$$E_{dip} = \vec{M}\left\langle \Phi \left| \frac{S(\vec{r},\epsilon)}{r^3}\left[\vec{\mu} - \frac{3(\vec{\mu}\cdot\vec{r})\cdot\vec{r}}{r^2} \right] \right| \Phi \right\rangle. \tag{2}$$

Here, $S(\vec{r},\epsilon) = \{1 + [\epsilon - V(\vec{r})]/2mc^2\}^{-1}$ is the reciprocal of the electronic relativistic mass enhancement, $\vec{L}$ and $\vec{\mu}$ are the operators of electronic angular moment and spin magnetic moment respectively, ϵ is the electronic energy, $V(\vec{r})$ is crystalline potential, and $\vec{M}$ is the nuclear magnetic moment. Averaging is performed using the large component $|\Phi\rangle$ of crystalline four-component wave function, which is an eigenspinor of the Dirac Hamiltonian without the hyperfine interaction term included.

In order to show how the MHF can arise from the nonmagnetic In $5p$ shell, we will use qualitative arguments. In the FP-LAPW method, the crystalline wave function is expanded in terms of electronic orbitals inside the atomic spheres. The calculation of the orbital and spin-dipolar fields coming from the $5p$ shell of In thus involves summation over the relevant terms in Eqs. (1) and (2) with p_x, p_y, and p_z characters both for spin up and spin down direction. To obtain the contribution from the $5p$ shell in the case of spin-dipolar field, for example, the following sum should be considered:

$$\sum_{i,i'} \sum_{\sigma,\sigma'} \langle \Phi^{\sigma}_{p_i} | T(\vec{r},\epsilon)\cdot\vec{\mu} | \Phi^{\sigma'}_{p_{i'}} \rangle \{i, i' = x,y,z\}, \{\sigma,\sigma' = \uparrow,\downarrow\}, \tag{3}$$

where $T(\vec{r},\epsilon)$ is a weighting function, which depends on the electronic position and energy, the form of which can be easily deduced from Eq. (2). After averaging, which involves integration over volume and energy, each of the terms in the above sum will produce a different number for the dipolar field. In the absence of the weighting function ($T = 1$), these numbers would cancel each other, since the $5p$ shell has the resultant spin equal to zero. As can be seen in Fig. 3, the energy distribution of spins is different for each subshell and the same is true for their spatial distribution. Due to these differences, the terms in expression (3) do not cancel each other and a nonzero spin-dipolar field arises at the In nucleus. The MHF induced in this manner has a transferred field character since its source, the In $5p$ subshells polarization, is created through the interaction with the magnetic Ce atoms.

It may be interesting to discuss the above FP-LAPW results in view of a recently proposed criterion for the appear-

ance of an induced magnetic moment on a diamagnetic atom in a magnetic crystal.[16,23] The latter is based on the symmetry analysis of the magnetic structures of the moment-inducing sublattice and the moment-induced sublattice. According to this criterion, a magnetic moment should always appear at the moment induced sublattice whenever it is allowed by symmetry. An analysis of this type has been performed recently in the UIn_3 system in Ref. 24 and it has been shown that indeed a small induced magnetic moment is developed on In if the compound is assumed to have a noncollinear magnetic structure with spin-orbit interaction taken into account. This effect comes through a small spin polarization of the valence $5s$ shell of In. Since UIn_3 and $CeIn_3$ are isostructural, one could treat the case of $CeIn_3$ in an analogous manner. The induced nonzero magnetic moments should therefore appear at all In sites, having the directions that are noncollinear with the direction of the Ce magnetic moments, through spin polarization of $5s$ valence shell of In. As our approach is based on collinear magnetic structure the result of the calculation showed a completely nonmagnetic solution for In atoms.

The polarization of the In $5p$ subshells observed in the present calculation, however, is an effect that should not depend much on the mutual orientation of the Ce and In magnetic moments. In order to further check this point we, separately, performed a spin-polarized FP-LAPW calculation for $CeIn_3$ without including the spin-orbit coupling term in the Hamiltonian. In this case no direction for magnetic moments has to be specified. The results obtained for the In $5p$ shell were qualitatively the same as earlier, that is, one obtains a spin polarized $5p$ subshell, but a zero total spin moment for the $5p$ shell. We therefore believe that the polarization of the In $5p$ subshells should be expected even when a noncollinear ordering of the Ce and In magnetic moments, allowed by symmetry, is assumed. In other words, both contributions, namely, the $5p$ subshell polarization, as obtained in the present calculation, and the spin polarization of the In $5s$ shell expected from the noncollinear structure as suggested in Ref. 24, may coexist in $CeIn_3$. Although this latter contribution could not be deduced directly from the present calculations, the possibility of the existence of an additional MHF in $CeIn_3$ at the In position, due to the $5s$ shell polarization, can not be excluded at this point. However, to account for this effect, symmetry allowed noncollinear magnetic structures of the Ce and In sublattices have to be studied in more detail.

V. ELECTRIC HYPERFINE FIELDS

In $CeIn_3$ only the In nuclei, having a noncubic environment, exhibit the electric quadrupole interaction. This is the result of the interaction of the nuclear quadrupole moment Q, with the electric-field gradient (EFG) due to the other charges in the crystal. The EFG is obtained by applying the gradient operator to the electrostatic potential, at the nuclear position, produced by valence electrons inside the atomic sphere as well as by the rest of the charges in the crystal. By measuring the strength of this interaction one can obtain important information about the electronic ground-state properties through the EFG tensor, provided the quadrupole moment Q of the nucleus is known.

TABLE II. Main component of EFG tensor at In sites in $CeIn_3$ compound, from experiment (Ref. 9) and from present work. Decomposition of the valence contribution is given also. V_{zz} is given in the units of 10^{21} V/m^2.

	$\lvert V_{zz}\rvert$ experiment	V_{zz} FP-LAPW	Valence contr.	s-d contr.	p-p contr.	d-d contr.
In	11.6	12.49	12.54	−0.05	13.26	−0.67

The EFG tensor being symmetric and traceless can always be diagonalized, and completely specified by two independent parameters: V_{zz}, the largest component of the EFG tensor and the asymmetry parameter η defined as $\eta=(V_{xx}-V_{yy})/V_{zz}$, where V_{xx}, V_{yy} and V_{zz} are the elements of EFG tensor in its principal axis system. These two quantities are usually determined from experiment. Table II shows the result of FP-LAPW calculation for V_{zz} at the In site. The asymmetry parameter η is zero due to the presence of a threefold symmetry axis. The experimental result is also shown in this table for comparison.

Practically all contribution to the EFG at In site originates from its valence electron shells. The $5p$ shell contribution is predominant, since the $4d$ shell of In is full and consequently spherically symmetric. A small d contribution shown in Table II results from an extension of the tails of the wave functions arriving from another atomic spheres into the In atomic sphere.

In the previous section it was shown that In nuclei exhibit nonzero MHF in $CeIn_3$ due to small spin polarization of the In $5p$ subshells. In order to further investigate the effect of this polarization on EFG we calculated the EFG tensor for spin up and spin down charge densities separately. The results did not show any difference between V_{zz}-up and V_{zz}-down values. Moreover, further decomposition into s-d, p-p, and d-d contribution is also the same for spin up and spin down configurations. It may be concluded therefore that polarization of $5p$ subshells does not influence the In EFG. The explanation follows from the analysis of DOS of In $5p$ subshells shown in Fig. 3 from which it is clear that the differences between spin up and spin down states appear only in the vicinity of the Fermi level. The occupied parts of bands with lower energies remain unpolarized. If we consider not only the energy dependence of the wave functions but also their spatial distribution, it is reasonable to assume that the low-energy DOS correspond to the parts of wave functions which are closer to the nucleus (since the Coulomb potential is deeper in this region). This is also the most important region for the formation of EFG, since the first node of the $5p$ wave function is situated in this region.[25] An integration over this region produces the major part of the EFG, and since in this region there is no polarization, V_{zz}-up and V_{zz}-down values are the same. The small differences between up and down wave functions do appear in the region far from nucleus (closer to the Fermi level) but they do not significantly change the EFG value. The V_{zz} value obtained after integration up to the radius of just 0.823 a.u. is only less

than 1% different from the V_{zz} value calculated from the integration up to 3.0 a.u.

VI. CONCLUSIONS

The $CeIn_3$ intermetallic compound can be described as a concentrated Kondo system in which Ce magnetic moments are ordered antiferromagnetically at very low temperatures. In order to study hyperfine interactions and to provide an interpretation of the recent experimental data, the first-principles FP-LAPW calculations of $CeIn_3$ in its antiferromagnetic phase have been performed. Spin-orbit interaction has been included in the calculations and $4f$ states of Ce have been treated as band states. A metallic solution for the electronic structure has been obtained with large DOS at the Fermi level originating mostly from Ce $4f$ states. A final result was a perfect antiferromagnetic ordering of Ce moments, while In atoms remained completely nonmagnetic. Three independent calculations, differing in the assumed direction of the Ce magnetization axis only, gave almost identical results. It was thus not possible to determine a preferable direction for the Ce magnetic moment. In all calculations the magnetization axes of In and Ce were considered to be collinear.

The calculations showed that the important states of the Ce atom, apart from $4f$ are $6s$, $6p$, and $5d$ states. They are positioned around the Fermi level with DOS overlapping with the $4f$ shell DOS. All of them are spin polarized due to interaction with magnetic moment of the $4f$ shell. The In atom has $5s$ and $5p$ states in the conduction band, while the $4d$ states remained corelike. Both the $5s$ and $5p$ shell of In have zero magnetic moment. However, each $5p$ subshell carries a nonzero spin magnetic moment although these moments cancel each other to give a net zero value for the p shell moment. Energy distributions of spin up and spin down $5p$ subshell states show differences only in the vicinity of the Fermi level, unlike the states at lower energies. The polarization of In $5p$ subshells has been attributed to their hybridization with extended spin-polarized Ce valence states.

The MHF at the Ce position is dominated by the orbital contribution mostly coming from the $4f$ shell. The contact field is very small due to an almost complete cancellation of the valence and core-electrons contributions. The $4f$ orbital field calculated for Ce in the $CeIn_3$ is in complete disagreement with the free Ce^{3+} ion value indicating that the $4f$ shell of Ce changes significantly in $CeIn_3$ compound.

Both the MHF and EFG at In position originate from the $5p$ shell. A small value of MHF is the consequence of different energy and spatial distribution of spins in $5p$ subshells. On the other hand, EFG is generated in a way typical for most hexagonal close packed metals, i.e., by the integration over a region close to the nucleus where the $5p$ wave function exhibits the first node. The polarization of the $5p$ subshells does not influence the EFG since it does not occur in the region, close to the nucleus, which is important for the EFG formation.

ACKNOWLEDGMENTS

Partial support for this research was provided by the Fundação de Amparo à Pesquisa do Estado de São Paulo (FAPESP). M.V.L. thankfully acknowledges financial support from FAPESP. Computer resources provided by Laboratório de Computação Científica Avançada da Universidade de São Paulo are thankfully acknowledged. We also wish to express our sincere thanks to Professor Sonia Frota-Pessôa for helpful discussion.

*On leave from Institute of Nuclear Sciences 'Vinča', PO Box 522, 11001 Belgrade, Yugoslavia.

†Corresponding author. Email address: jmestnik@net.ipen.br

[1] K. H. J. Buschow, Rep. Prog. Phys. **42**, 1373 (1979).

[2] G. R. Stewart, Rev. Mod. Phys. **56**, 755 (1984).

[3] S. Rahman, J. Timlin, J. E. Crow, T. Mihalisin, and P. Schlottmann, J. Appl. Phys. **67**, 5209 (1990).

[4] J. M. Lawrence and S. M. Shapiro, Phys. Rev. B **22**, 4379 (1980).

[5] J. Lawrence, Phys. Rev. B **20**, 3770 (1979).

[6] J. Flouquet, P. Haen, P. Lejay, P. Morin, D. Jaccard, J. Schweizer, C. Vettier, R. Fisher, and N. E. Phillips, J. Magn. Magn. Mater. **90-91**, 377 (1990).

[7] A. W. Carbonari, J. Mestnik-Filho, R. N. Saxena, and H. Saitovitch, Hyperfine Interact **133**, 77 (2001).

[8] H. Saitovitch (private communication).

[9] Y. Kohori, Y. Inoue, T. Kohara, G. Tomka, and P. C. Riedi, Physica B **259-261**, 103 (1999).

[10] R. Vianden, Hyperfine Interact. **15/16**, 1081 (1983).

[11] O. K. Andersen, Phys. Rev. B **12**, 3060 (1975).

[12] A. Benoit, J. K. Boucherle, P. Convert, J. Flouquet, J. Palleau, and J. Schweizer, Solid State Commun. **34**, 293 (1980).

[13] P. Blaha, K. Schwarz, and J. Luitz, *WIEN97, A Full Potential Linearized Augmented Plane Wave Package for Calculating Crystal Properties* (Tech. Univ. Wien, Vienna, 1999), ISBN 3-9501031-0-4. Updated version of P. Blaha, K. Schwarz, P. Sorantin, and S. B. Trickey, Comput. Phys. Commun. **59**, 399 (1990).

[14] J. P. Perdew, K. Burke, and M. Ernzerhof, Phys. Rev. Lett. **77**, 3865 (1996).

[15] S. Blügel, H. Akai, R. Zeller, and P. H. Dederichs, Phys. Rev. B **35**, 3271 (1987).

[16] L. M. Sandratskii and J. Kübler, Phys. Rev. B **60**, R6961 (1999).

[17] J. P. Perdew and A. Zunger, Phys. Rev. B **23**, 5048 (1981).

[18] V. I. Anisimov, J. Zaanen, and O. K. Andersen, Phys. Rev. B **44**, 943 (1991).

[19] A. J. Freeman and R. E. Watson, in *Magnetism*, edited by G. T. Rado and H. Suhl (Academic, New York, 1965), Vol. 2A.

[20] M. Forker, Hyperfine Interact. **24-26**, 907 (1985).

[21] R. G. Barnes, in *Handbook of the Physics and Chemistry of Rare Earths*, edited by K. H. Gschneider, Jr. and L. R. Eyring (North-Holland, Amsterdam, 1979).

[22] R. Selim and T. Mihalisin, Solid State Commun. **59**, 785 (1986).

[23] L. M. Sandratskii, Adv. Phys. **47**, 91 (1998).

[24] S. Demuynck, L. Sandratskii, S. Cottenier, J. Meersschaut, and M. Rots, J. Phys.: Condens. Matter **12**, 4629 (2000).

[25] P. Blaha, K. Schwarz, and P. H. Dederichs, Phys. Rev. B **37**, 2792 (1988).